PHYSICAL REVIEW B VOLUME 28, NUMBER 8 15 OCTOBER 1983

Epitaxy and thick-film formation on an attractive substrate: The systematics of a lattice-gas model

C. Ebner
Department of Physics, The Ohio State University, Columbus, Ohio 43210

Craig Rottman and Michael Wortis
Department of Physics and Materials Research Laboratory, University of Illinois at Urbana—Champaign, Urbana, Illinois 61801
(Received 11 May 1983)

A lattice-gas model consisting of an inert attractive substrate and an adatom gas with nearest-neighbor repulsion and next-nearest-neighbor attraction is studied by mean-field and Monte Carlo methods. Epitaxial (sublattice-ordered) phases appear in the surface phase diagram and it is possible to examine in this context the interplay between film formation (layering and wetting) and lateral ordering (epitaxy). For a given adatom/substrate pair, film buildup proceeds in the usual way, except that regions of epitaxy appear in the surface phase diagram. Strong enough substrate attraction produces high-density, compressed layers and quenches epitaxy. Because of the adatom-adatom nearest-neighbor repulsion, this compression can lead to a nonmonotonic dependence of wetting behavior on substrate strength and even to complete dewetting at $T=0$ for certain strong substrates. The relation of these phenomena to various experimental observations is discussed.

I. INTRODUCTION

When an attractive planar surface (the substrate) is exposed to a bulk gas (the absorbate), a region of locally enhanced particle density (the film) may form.[1-6] This film behaves as a two-dimensional system in equilibrium with the bulk gas. Its equilibrium structure is described by a nonuniform particle density $\langle n(z,\vec{\rho})\rangle$, where z measures distance from the substrate, $\vec{\rho}$ is the transverse coordinate, and the angular brackets denote a thermodynamic average. As $z\to\infty$, $\langle n(z,\vec{\rho})\rangle$ approaches the bulk-gas density n_b. The local excess surface density

$$n_s(\vec{\rho})=\int_0^\infty dz[\langle n(z,\vec{\rho})\rangle - n_b] \tag{1}$$

provides a useful measure of the transverse variation of the film. The average excess surface density

$$n_s=\lim_{S\to\infty}\frac{1}{S}\int_S (d^2\rho) n_s(\vec{\rho}) \tag{2}$$

(S is the total exposed surface area) measures the overall quantity of adsorbed material.[7] It is roughly proportional to the film thickness t provided that the density profile across the film is more or less uniform. Bulk properties like n_b may be regarded as depending on temperature T, chemical potential[8] μ, and the form of the adatom-adatom interactions, taken here to be described by a spherically symmetric pair potential $v(\vec{r})$. Surface properties like $\langle n(z,\vec{\rho})\rangle$, $n_s(\vec{\rho})$, n_s, etc., depend on these quantities plus the adatom/substrate interactions, here described by a single-particle potential $u(z,\vec{\rho})$.

Film structure has been studied—theoretically and experimentally—mainly in two limits. Much recent work focuses on the thin-film regime (monolayer and submonolayer), where n_b is small and surface-bulk coexistence ceases to play an important role, so the film may be regarded as a strictly (or effectively) two-dimensional system and $n_s(\vec{\rho})$ corresponds precisely to the areal density. There is a wealth of experimental data in this regime,[1-4] exhibiting a variety of phase transitions which involve changes in the lateral symmetry of $n_s(\vec{\rho})$. We mention in particular epitaxial transitions and the $d=2$ (incommensurate) solid—to—(commensurate)-fluid transition ("melting"). Physically these transitions are driven by competition (or frustration) effects and have been more or less successfully understood on the basis of $d=2$ models.[5] Another body of work[9-17] explores multilayer behavior and thick-film transitions, such as layering, wetting, prewetting, etc. In this region surface-bulk coexistence effects (such as desorption) are important and, for a given adatom/substrate pair, lateral symmetry and lateral ordering usually play secondary roles. Several models purport to elucidate this behavior.[9-17] None of them up to now has incorporated competing interactions and associated lateral-ordering effects.

The purpose of our work herein is to explore, albeit in a preliminary way and on the basis of a specific model calculation, the interplay between lateral ordering (epitaxy, in this example) and thick-film behavior. We are primarily motivated by the qualitative question: how does lateral ordering influence the systematics of film growth? The response seems to be that, for a given adatom/substrate pair, the gross systematics is not altered but that certain regions of the surface phase diagram, surrounded by appropriate phase boundaries (an "envelope of epitaxy" in our example), develop lateral order. A sufficiently strong substrate may quench the epitaxy in the first few layers. When this occurs, interlayer adatom-adatom repulsion weakens the effective attraction of the substrate and may even lead, under appropriate conditions, to incomplete wetting at coexistence. This behavior may provide a possible clue to the understanding of the results of recent re-

flection high-energy electron diffraction (RHEED) measurements[18] on Ne, N_2, Ar, and Xe on graphite. These systems, which form incommensurate solid layers at low temperatures, exhibit incomplete wetting when substrate attraction is strongest relative to adatom-adatom attraction (Ne and N_2) and complete wetting when it is weaker (Ar and Xe), contrary to the "usual" systematics.[12–15]

The plan of the paper is as follows. The remainder of this section is devoted to a qualitative discussion of the role of symmetry in surface-ordering phenomena, including the effect of surface-bulk coexistence. Section II A introduces a lattice-gas model sufficiently general to exhibit surface epitaxial ordering in the bulk-gas phase. Section II B describes the bulk properties of this model. Section II C covers its $T=0$ surface behavior, which may be treated exactly. Section III is devoted to surface calculations for $T>0$. Representative surface phase diagrams are exhibited, derived via meanfield theory and Monte Carlo simulations and showing a variety of layering and epitaxial transitions. Section IV summarizes the calculated behavior of the model and its relationship to both real epitaxial ordering and the wetting data mentioned above.

The thermodynamics of the surface region[6,14,19,20] is described by a well-defined free energy per unit surface area $f_s(T,\mu,v,u)$, distinct from but coexisting with the ordinary free energy per unit volume $f_b(T,\mu,v)$ of the bulk. The surface phase diagram consists of the loci of nonanalycity of f_s as a function of whichever of its variables are of interest (e.g., T and μ). The surface region exists as a sandwich, bounded on one side by the substrate and on the other by the bulk. Bulk phase transitions drive the surface region in a nonanalytic manner and, for this reason, the surface phase diagram contains, as a subset, the bulk phase boundaries. In addition, there may be phase boundaries due to ordering of the surface region alone, without concomitant bulk singularity. We focus here on phase transitions[5] associated with lateral ordering of the surface density $n_s(\vec{\rho})$. Assume for simplicity that the bulk phase remains fluid, so that the bulk density is spatially uniform.[7] The surface region is always subject to the periodicity of the substrate potential; thus, in the absence of additional, intrinsic surface ordering, $n_s(\vec{\rho})$ [and, indeed, $\langle n(z,\vec{\rho})\rangle$] has the symmetry of the substrate potential. Phase transitions occur whenever $n_s(\vec{\rho})$ develops a lower symmetry than that of the substrate. When the symmetry group of $n_s(\vec{\rho})$ changes to a subgroup of the symmetry group of the substrate, the transition is called "epitaxial"; otherwise, the transition is "commensurate-incommensurate."[21] The $d=2$ melting transition is of the latter type.[22,23] Note that the substrate potential continues to modulate the incommensurate phase. More or less complex sequences of such transitions can also occur. For example, He/graphite[24] at low T and for coverages near one third of a monolayer exists in an epitaxial $(\sqrt{3}\times\sqrt{3})$ phase. As the density is increased and the hard-core He-He repulsion pushes adatoms off the substrate-preferred adsorption sites, this epitaxial phase gives way to an incommensurate $d=2$ solid phase. The lattice-gas model introduced below lends itself well to the study of epitaxial transitions but poorly to the study of commensurate-incommensurate transitions.[25]

II. LATTICE-GAS MODEL WITH MIXED INTERACTIONS

A. Model

We consider a lattice gas of the type originally proposed for adsorption by de Oliveira and Griffiths,[11] only with nearest-neighbor (NN) and next-nearest-neighbor (NNN) interactions of opposite sign. The Hamiltonian (including the chemical-potential term) is

$$H-\mu N=v_1\sum_{\substack{\langle ij\rangle\\ \text{NN}}} n_i n_j - v_2\sum_{\substack{\langle ij\rangle\\ \text{NNN}}} n_i n_j+\sum_i (u_i-\mu)n_i,\quad n_i=0,1\ . \tag{3}$$

The lattice is simple cubic and semi-infinite consisting of layers $z=1,2,\ldots$. We shall choose the energy parameters v_1 and v_2 to be non-negative; hence there is soft NN repulsion ($v_1<\infty$) and NNN attraction, while the lattice supplies hard-core exclusion. The substrate potential, represented by u_i, is attractive and typically decays monotonically with z. We shall write

$$u_i=-uf_z \tag{4a}$$

for i in layer z, where $u>0$ is an energy parameter and $f_1\geq f_2\geq\cdots\geq 0$. In calculations we shall use

$$f_z=\begin{cases}7.85\ , & z=1\\ 4.2/z^3\ , & z>1\ .\end{cases} \tag{4b}$$

It is useful to define the dimensionless ratios

$$R\equiv v_1/v_2\ ,\quad \alpha\equiv u/v_2\ ,\quad \beta\equiv u/v_1\ . \tag{5}$$

When $\alpha=1$, the surface potential u_i reduces to that used by de Oliveira and Griffiths.[11]

By transforming to Ising variables, $n=\frac{1}{2}(1+\sigma)$, $\sigma=\pm 1$, it is easy to verify that this model has certain useful symmetries.[14] We write

$$\begin{aligned}\mu&=3v_1+6v_2+\Delta\mu\ ,\\ u_1&=\tfrac{1}{2}v_1+2v_2+\Delta u_1\ ,\\ u_z&=\Delta u_z\ ,\quad z>1\ .\end{aligned} \tag{6}$$

The model is then symmetric under

$$v_{1,2}\leftrightarrow v_{1,2}\ ,\quad \Delta\mu\leftrightarrow-\Delta\mu\ ,\quad \Delta u_z\leftrightarrow-\Delta u_z \tag{7}$$

(this is just the usual magnetic symmetry $\sigma\leftrightarrow-\sigma$) and for $\Delta\mu=\Delta u_z=0$ (only) under

$$v_1\leftrightarrow-v_1\ ,\quad v_2\leftrightarrow v_2 \tag{8}$$

(this is the two-sublattice antiferromagnetic symmetry, $\sigma\leftrightarrow-\sigma$ in sublattice A and $\sigma\leftrightarrow\sigma$ in sublattice B).

B. Bulk behavior

Figure 1 shows how the bulk phase diagram varies with R. For $v_1=0$ ($R=0$) the two interpenetrating fcc sublattices are independent and align ferromagnetically at sufficiently low temperatures. This corresponds to first-order gas-liquid condensation at $\mu=-6v_2$ with a critical temperature[26] $k_BT_c=2.449v_2$. The effect of a nonzero v_1 is

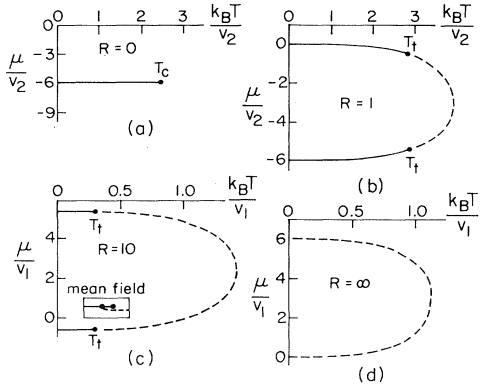

FIG. 1. Bulk $d=3$ phase diagrams for a variety of antiferromagnetic-to-ferromagnetic ratios $R=v_1/v_2$. First-order phase boundaries are drawn with solid lines; second-order phase boundaries are dotted. $R=1$ and 10 phase boundaries are from our Monte Carlo data. Inset for $R=10$ shows the topology (not to scale) of the critical-endpoint structure exhibited by the mean-field approximation for $R>\frac{10}{3}$. $R=\infty$ data are given in Refs. 27 and 28.

to suppress simultaneous occupation of NN sites. When $v_2=0$ ($R=\infty$), the lattice gas has an "antiferromagnetic" regime at low temperatures, where one sublattice is preferentially occupied. This regime extends from $\mu=0$ to $6v_1$ at $T=0$, reaches a maximum temperature of[26] $k_BT_c=1.128v_2$ at $\mu=3v_1$, and is surrounded by a second-order phase boundary.[27,28] We note in passing that mean-field theory[29–31] leads to an $R=\infty$ phase diagram with a noticeable bulge at $T=0$, so that the lines $\mu=0$ and $\mu=6v_1$ intersect the phase boundary both at $T=0$ and, again, at $T>0$. It is evident in Fig. 1(d) that this effect is strongly suppressed by fluctuations, and the low-temperature phase boundary is nearly parallel to the T axis.[32] When both v_1 and v_2 are nonzero, sublattice order persists with a phase diagram which is symmetric about $\mu=3v_1-6v_2$ [Eq. (6)]. At high temperature the phase boundary is second order and reaches a maximum which scales roughly as $\frac{3}{2}v_1+3v_2$ (mean-field theory).[29–31] At low temperature it is first order and terminates at $T=0$, $\mu=6(v_1-v_2),-6v_2$. The first- and second-order regions of the phase boundary meet at a temperature T_t which scales to zero linearly with v_2 (at fixed v_1) to recover the $R=\infty$ limit. For small R the antiferromagnetic region becomes very narrow in the μ direction, the second-order part of the phase boundary shrinks, and the two points T_t coalesce to become the (pure) ferromagnetic T_c.

Certain details of the behavior near T_t are not completely pinned down at present.[33] We regard it as likely that T_t is, for all $0<R<\infty$, an ordinary tricritical point, where the first- and second-order parts of the phase boundaries join with no slope change. This phenomenology contradicts mean-field theory,[29–31] which predicts a changeover from a tricritical point for $R<R_c=\frac{10}{3}$ to a critical-endpoint structure for $R>R_c$, in which the second-order boundary sweeps outside the first-order boundary and joins it with a discontinuity in slope, leaving a small first-order spur inside the antiferromagnetic region (see $R=10$ inset). In the corresponding $d=2$ model, it is generally accepted that fluctuations wipe out this effect.[32] For $d=3$, however, some remnants of this behavior seem to persist at large R: Careful Monte Carlo studies at $R=10$ and 20 (Sec. III A) show rapid but apparently smooth small slope changes[34] near T_t; however, no first-order spur is detectable. Herrmann *et al.*[33] observe anomalous behavior of effective exponents, but overall their evidence is not inconsistent with ours. If any critical-endpoint structure exists for large R, its scale must be very small, indeed. In any case, this is not a region of the phase diagram with which we shall be deeply concerned in the surface studies which follow.

The bulk properties described above are evidently quite different from those of a three-phase continuum gas-liquid-solid system (Fig. 2). We shall argue, nevertheless, that *in an appropriate regime* the surface behavior of our lattice model can mimic many of the properties of real epitaxial adsorption. The difficulty is bulk sublattice order, which exists in our model as an artifact of the imposed structure but is wiped out in the continuum system by entropic effects, since the interparticle spacing can adjust continuously. Thus, the first-order part of the model phase boundary, driven principally by the attractive interaction v_2, is physical and has as its counterpart real gas-solid—gas-liquid condensation (this lattice model[35] does not distinguish between the two high-density phases); however, the second-order part of the model phase boundary and the sublattice ordering beyond it lack continuum counterparts. The situation at the surface is somewhat different, because the lattice does plausibly model[36] the periodicity of the preferred adsorption sites offered by the substrate and described in the continuum picture by the lateral modulation of $u(z,\vec{\rho})$. Thus, surface-phase sublattice order, which we shall study below, has epitaxy as its physical counterpart. On the other hand, the two-dimensional "liquid-solid" (melting) transition, in which particles move out of "registry" into positions incommensurate with the substrate, has no analog in this lattice model.[25,35]

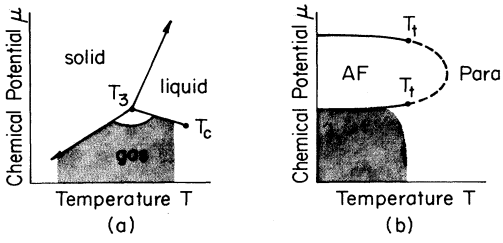

FIG. 2. Comparison of the bulk phase diagrams of (a) the continuum gas-liquid-solid system and (b) our lattice gas with competing interactions. The lattice gas has only two phases and lacks a triple point. The continuum system has no extended second-order phase boundary. However, surface behavior in the shaded regions may be analogous, as explained in the text.

C. Surface behavior at $T=0$ (exact)

The state of the system at $T=0$ and fixed chemical potential μ is determined by finding the ground state of the Hamiltonian (3). Such calculations are straightforward and the results show interesting structure. The relevant (low-energy) states are made up of a sequence of homogeneous layers, each one of which is empty (denoted "0"), full ("1"), or ordered ("A") with one full and one empty sublattice. Interactions act only between adjacent layers. Table I gives the contribution per unit area to the $T=0$ free energy (3) for each type of layer and for each type of adjacent-layer pair. One reads off the bulk free energy per site for the three pure phases,

$$f_b^{(0)}(\mu)=0\ ,\quad f_b^{(A)}(\mu)=-3v_2-\tfrac{1}{2}\mu\ ,$$
$$f_b^{(1)}(\mu)=3v_1-6v_2-\mu\ . \tag{9}$$

Minimization gives $f_s(\mu,T=0)$ and the $T=0$ phase boundaries of Fig. 1. We shall specify nonuniform configurations in the form $[1^k0^lA^m\cdots]$ (layers $z=1,\ldots,k$ full; layers $z=k+1,\ldots,k+l$ empty; layers $z=k+l+1,\ldots,k+l+m$ ordered; etc.), stopping when the uniform bulk is attained. Relevant low-energy configurations for the potentials (4) when the bulk is gas (empty) are [0], $[1^n]$, $[A^n]$, $[1^nA^m]$, and $[1^n0A^m]$. Corresponding surface free energies per unit area are easy to read off. For example, for bulk gas and $n>0$,

$$f_s^{(1^n)}(\mu)=(3n-1)v_1-(6n-4)v_2+\sum_{\nu=1}^{n}(u_\nu-\mu)\ . \tag{10}$$

Minimization at each μ over the various trial surface configurations identifies the physical configuration and its free energy $f_s(\mu,T=0)$.

The sequence of ground-state configurations which the system passes through as μ varies may be quite complex. As an example, Fig. 3 shows the β, μ phase diagram for the purely antiferromagnetic case $v_2=0$ with the substrate potentials (4) and (5). It is a special feature of the case $v_2=0$ that many of the $T=0$ phase boundaries disappear immediately when T is raised above zero. Those that remain for $T>0$ are all second-order and include only (i) the bulk phase boundaries, and (ii) those other phase boundaries involving a change of order, i.e., those separating a state with only 0 and 1 layers and a state with one or more A layers. A diagnostic of this situation is the energy cost of *local* opposite-phase fluctuations (nucleation) at the phase boundary. When these fluctuations have no cost (as at $v_2=0$), then phase boundaries which couple to ordering are second order for $T\gtrsim 0$ and the rest disappear. For

TABLE I. Contributions to the $T=0$ free energy [Eq. (3)] per unit substrate surface area. Layer pairs [0X] contribute nothing.

Layers		Layer pairs	
[0]	0	[AA]	$-2v_2$
[A]	$\frac{1}{2}(u_z-\mu)-v_2$	[A1]	$\frac{1}{2}v_1-2v_2$
[1]	$(u_z-\mu)+2(v_1-v_2)$	[11]	v_1-4v_2

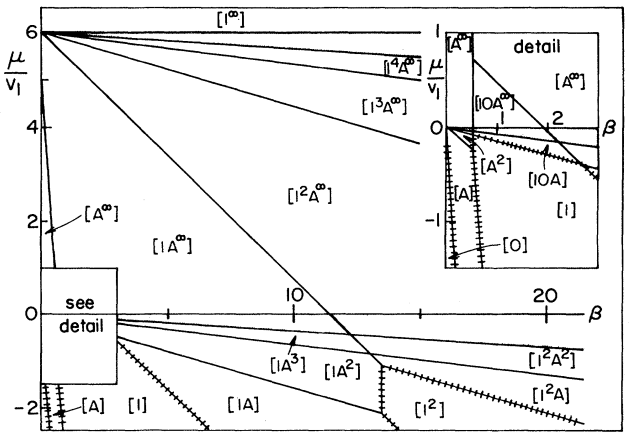

FIG. 3. $T=0$ surface phase diagram for the purely antiferromagnetic (repulsive) case $R=\infty$. The parameter $\beta\equiv u/v_1$ [Eq. (5)] measures the ratio of the substrate strength to the interparticle repulsion. Square brackets label different phases according to the convention explained in the text. Narrow shaded regions contain infinite sequences of additional phase boundaries. Barred lines indicate boundaries between regions with and without sublattice order and continue for $T>0$. Inset shows additional detail near the origin.

$v_2>0$, on the other hand, local nucleation has a nonzero energy cost and all $T=0$ phase boundaries survive as first-order transitions at sufficiently low nonzero T.

Another question which can be explored exactly at $T=0$ concerns the presence or absence of complete wetting and other related coexistence phenomena.[9–17] The issue here is the extent of film growth near coexistence. Consider, for example, $T=0$, $\mu\lesssim -6v_2$, in the bulk-gas phase but near the phase boundary (Figs. 1 and 2). Under appropriate circumstances a thick film with the structure $[\cdots A^n]$ may form, with $n\to\infty$ as $\mu\to -6v_2^-$ (coexistence), so that the film thickness t and the excess surface density n_s both diverge as μ approaches coexistence from below.[37] Figure 4 plots as a function of R and α [Eq. (5)] the structure of the film at $T=0$, $\mu=-6v_2^-$ (the gas side of the bulk coexistence boundary) for potentials of the form (4). Wetting is incomplete at coexistence for

$$\alpha<4\left[\sum_{\nu=1}^{\infty}f_\nu\right]^{-1}=0.4598\ldots\ ,$$

and in the triangular region [10^∞], where a single full layer without any overlayers is the lowest-energy configuration. This structure can lead to a sequence of wetting and dewetting transitions, as α (the substrate strength) is increased from zero for fixed R. For example, for $R=10$ incomplete wetting changes to complete at $\alpha=0.4598$, back to incomplete at $\alpha=6.2844$, and finally again to complete at $\alpha=11.784$. Such dewetting for strong substrates cannot occur for purely attractive adatom-adatom interactions.[13,14] The mechanism is as follows: When the first layer fills ($A\to 1$), then all second-layer sites are subject to NN repulsion. When v_1 is large enough, this

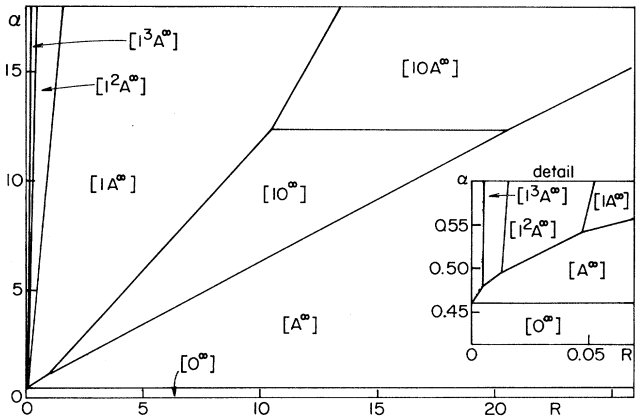

FIG. 4. Gas-phase surface behavior at $T=0$ in the coexistence limit $\mu\to -6v_2^-$. Designation $[\cdots A^\infty]$ indicates the formation of an infinitely thick (complete-wetting) film as coexistence is approached from the gas phase. Weakly attractive substrates ($\alpha<0.4598$) exhibit incomplete wetting. The mechanism for incomplete wetting by strongly attractive substrates $[10^\infty]$ is described in the text. The shaded region at small R and large α contains many additional boundaries.

depopulates the second-layer $[10\cdots]$. Subsequent layers can only fill when the substrate becomes strong enough to repopulate the second layer $[1A^\infty]$ or to overcome the energy cost of an $0A$ "interface" $[10A^\infty]$. Thus, a compact ("compressed") filling of early layers on a strong substrate can actually inhibit wetting, a point to which we shall return in Sec. IV in connection with the RHEED data[18] mentioned in the Introduction.

A $T=0$ coexistence phase diagram like Fig. 4 can be constructed on the opposite side of coexistence $\mu=-6v_2^+$, where complete drying,[14,38] $n_s\to\infty$, corresponds to configurations of the form $[\cdots 0^n]$, $n\to\infty$. Similarly, there may be complete wetting at $\mu=(6v_1-6v_2)^-$ (with configurations $[\cdots 1^\infty]$) and complete drying at $\mu=(6v_1-6v_2)^+$ with configurations $[\cdots A^\infty]$).

III. SURFACE BEHAVIOR FOR $T>0$

A. Methods

This section contains a few technical comments on the methods of calculation used. Mean-field theory[11,14,15,39–41] provides a quick and useful guide to systematics, provided its deficiencies are understood and compensated.[42] Monte Carlo calculations, accurate and reliable but much more time consuming, are used sparingly to check important points.

1. Mean-field theory

Mean-field theory for the lattice-gas model (3) may be obtained from the variational functional[43]

$$\mathscr{F}[\rho_i]=\sum_i\{k_BT[\rho_i\ln\rho_i+(1-\rho_i)\ln(1-\rho_i)]+(u_i-\mu)\rho_i\}+v_1\sum_{\substack{\langle ij\rangle\\ \text{NN}}}\rho_i\rho_j-v_2\sum_{\substack{\langle ij\rangle\\ \text{NNN}}}\rho_i\rho_j\ . \tag{11}$$

At the global minimum of (11), the local particle density is $\langle n_i\rangle\equiv\rho_i^{\min}$ and the free energy of the sample is $F=\mathscr{F}[\rho_i^{\min}]$ (mean-field approximations). We assume a two-sublattice structure ($k=A,B$) and allow for layerwise inhomogeneity ($z=1,2,\ldots$). The stationarity condition $\partial\mathscr{F}/\partial\rho_i=0$ leads to mean-field equations,

$$\rho_z^k=g(\epsilon_z^k)\ ,$$

with

$$\epsilon_z^{A,B}=u_z+v_1(\rho_{z-1}^{A,B}+4\rho_z^{A,B}+\rho_{z+1}^{A,B})-4v_2(\rho_{z-1}^{B,A}+\rho_z^{B,A}+\rho_{z+1}^{B,A})\ , \tag{12}$$

where

$$g(\epsilon)\equiv(e^{(\epsilon-\mu)/k_BT}+1)^{-1}\ . \tag{13}$$

This reduces in the bulk (b) to[29–31]

$$\rho_b^k=g(\epsilon_b^k)\ \text{ with }\epsilon_b^{A,B}=6v_1\rho_b^{A,B}-12v_2\rho_b^{B,A}\ . \tag{14}$$

Equation (12) is subject to boundary conditions $\rho_{z=0}^k=0$ and $\rho_{z=\infty}^k=n_b^k$ (the bulk sublattice density).

In practice we have solved Eqs. (12) and (14) by iteration, starting from initial guesses for ρ_b^k and $\{\rho_z^k\}$ and in the inhomogeneous case setting $\rho_z^k=n_b^k$ for $z\geq 10$. Different initial guesses can lead to different solutions of the mean-field equations. The one which makes the variational functional (11) smallest is selected as the global minimum. In principle there is, of course, a difficulty: Only those solutions of the mean-field equations which are *stable* under iteration can be found by this technique, and there is no proof of which we are aware that the physical solution is of this type. An alternative but numerically slower approach, which does not suffer from this uncertainty, is direct multivariable minimization of the free-energy functional (11). In selected checks minimization of (11) by the method of conjugate gradients[44] has always led us to the same solution as that obtained by the iterative method, so we believe that in practice the physical solution is iteratively stable.

2. Monte Carlo simulations

Monte Carlo techniques used are described in Ref. 45, only with one important improvement: We calculated the grand free energy per unit substrate surface area $\omega(T,\mu)$. Assume that the free energy is known at some reference point $\omega(T_0,\mu_0)$. To find $\omega(T,\mu)$ it is necessary to collect Monte Carlo data on the overall particle density $[n(T,\mu)\equiv\sum_z\langle n(z,\vec{\rho})\rangle$, averaged over $\vec{\rho}$] and energy density $[\epsilon(T,\mu)]$ per unit area along a path C connecting (T_0,μ_0) and (T,μ). Standard thermodynamic manipulations then give (in units such that $k_B=1$)

$$\omega(T,\mu)=\frac{T}{T_0}\omega(T_0,\mu_0)-T\int_C dl'\left[\frac{dT'}{dl'}g(l')+\frac{d\mu'}{dl'}y(l')\right]\ , \tag{15}$$

where $g=(\epsilon-\mu n)/T^2$, $y=n/T$, and dl' is an element of the path C. By calculating ω in this way for the various phases, it is possible quite accurately to locate first-order

phase boundaries, which are masked by metastability in standard Monte Carlo simulations. As a byproduct, one may obtain from $\omega(T,\mu)$ the entropy per unit area and, therefore, the latent heat of the first-order transitions.

Monte Carlo simulations for the bulk were carried out on periodically connected samples up to $20\times20\times20$. For the surface we used a slab geometry $L\times L\times D$ with periodic connectivity only in the transverse directions. The thickness of the slab ranged up to $D=15$, while the transverse dimension ranged from $L=20$ far from criticality up to $L=60$, necessary for precise location of tricritical points and critical temperatures for layering, wetting, and epitaxy.

Estimates of typical uncertainties in phase boundaries ($R=1,10$) are, for critical temperatures, $\pm0.03v_2/k_B$ (from size dependence) and, for first-order transitions, $\pm0.005v_2/k_B$. The latter figure arises from uncertainty in $\omega(T,\mu)/T$ of about $\pm0.003v_2$, which reflects both size and path dependence.

B. Limiting cases: $R=0,\infty$

A discussion of surface behavior when $R=0$ ($v_1=0$) and $R=\infty$ ($v_2=0$) will serve to bracket the more complex behavior occurring for $0<R<\infty$, treated in Sec. III C.

Surface systematics for purely attractive interactions ($R=0$) have been worked out recently by a number of groups using mean-field,[11,14,15,39,40,46] Monte Carlo,[45,47] and renormalization-group[48,49] techniques. Lattices studied have included simple cubic, hexagonal, and fcc. The systematics is sketched in Fig. 5. For sufficiently strongly attractive substrates [$\alpha\equiv u/v_2>\alpha_W=0.4598$ (fcc), Figs. 5(c) and 5(d)], there is an infinite sequence of first-order layer transitions, terminating at $T=0$, with distinct critical temperatures $T_c(n)$ approaching the interfacial roughening temperature T_R as $n\to\infty$. At $T=0$ the film structure is [1^n] and may be calculated exactly, as described in Sec. II C. Wetting is complete at coexistence for all $T<T_c$. For large enough α [$\alpha>0.5461$, Fig. 5(d)], the layer transitions are all disjoint. As α decreases [$0.5461>\alpha\to\alpha_W$, Fig. 5(c)], the early-layer transitions coalesce successively at low temperatures via a sequence of surface triple points.[50] When α decreases beyond α_W, a wetting temperature appears with complete wetting at coexistence above but not below T_W. So long as T_W is less than T_R [$\alpha_S>\alpha>\alpha_R$, Fig. 5(b)], distinct layer transitions remain.[50] When α is weakened still further ($\alpha_R>\alpha>\alpha_W$), $T_R<T_W<T_c$ and the layer transitions can no longer remain distinct at coexistence. At first the layer transitions are replaced by a single prewetting-transition line [Fig. 5(a)]. The length of this line goes to zero before T_W reaches T_c, leading to a regime of critical wetting.[14–17] For still weaker substrates ($\alpha_c>\alpha>0$), the gas side of bulk coexistence is incompletely wet at all $T<T_c$ but a drying transition[14,38] appears on the high-density side of coexistence.

In the opposite limit bulk interactions are purely repulsive ($v_2=0$, $R=\infty$) and the strength of the substrate potential is measured by $\beta\equiv u/v_1$. The lack of particle-particle attraction suppresses all layer transitions at $T>0$ (see Sec. II C); however, surface attraction produces a dense region near the substrate which can undergo epitaxial (antiferromagnetic) ordering before the bulk transition. Representative mean-field surface phase diagrams are shown in Fig. 6. The corresponding results corrected for fluctuations are given in Fig. 7 for comparison. The main visible effects of fluctuations are to reduce T_c and to suppress the characteristic low-temperature bulge of the mean-field phase boundaries (Sec. II B). For $\beta=0$ ($u=0$) there is no region of surface (as opposed to bulk) sublattice order. As soon as u becomes positive, a small epitaxially ordered surface region appears near $T=\mu=0$. This region grows with u. At $\beta=4/(f_1-f_2)=0.5461$, an island of disorder first appears near $T=0$ (e.g., $\beta=0.62$). The island grows, as u increases further, and the ordered region stretches and eventually divides into two disjoint subregions (e.g., $\beta=1.0$). A second disordered island ap-

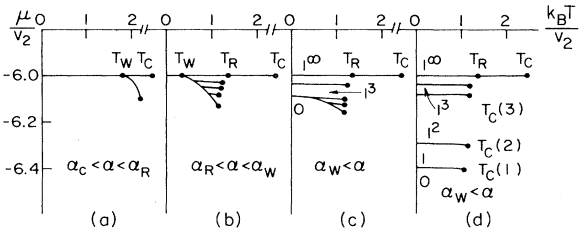

FIG. 5. Surface phase diagrams for $R=0$ ($v_1=0$), which corresponds to an fcc lattice with NN attractive adatom-adatom interactions. The parameter $\alpha=(u/v_2)$ measures the strength of the adatom-substrate attraction and increases from left to right. In (b)–(d) there is an infinite sequence of layer transitions approaching bulk coexistence (only four of which can be shown on the scale of the figure). For $R=0$, $\alpha_W=0.4598$. Intercepts at $T=0$ are correct for (c) $\alpha=0.500$ and (d) $\alpha=0.560$.

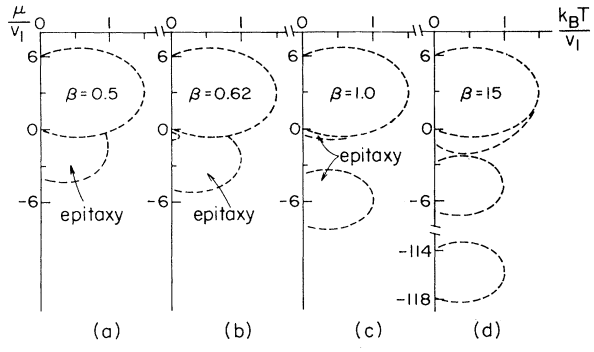

FIG. 6. Mean-field surface phase diagrams for $R=\infty$ ($v_2=0$). The parameter $\beta=u/v_1$ measures the strength of the adatom-substrate attraction and increases from left to right. Upper boundary encloses the bulk "antiferromagnetic" phase [cf. Fig. 1(d)] and does not change with β. As β increases, regions of epitaxial (surface) order split off from the bulk phase boundary. Each region forms as a layer becomes (roughly) half-filled, and then quenches as filling is completed. Behavior at $T=0$ is given exactly by mean-field theory.

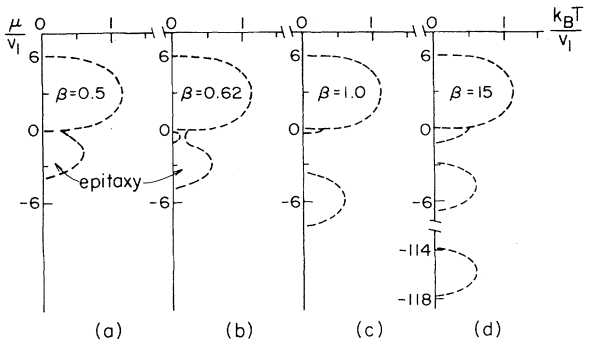

FIG. 7. Surface phase diagrams for $R=\infty$ ($v_2=0$) beyond mean-field theory. Note, by comparison with Fig. 6, the decrease in T_c and the disappearance of the mean-field bulge. The bulk phase boundary is the same as Fig. 1(d). Separated regions of (surface) epitaxy closely resemble $d=2$ simple quadratic phase boundaries (Ref. 32).

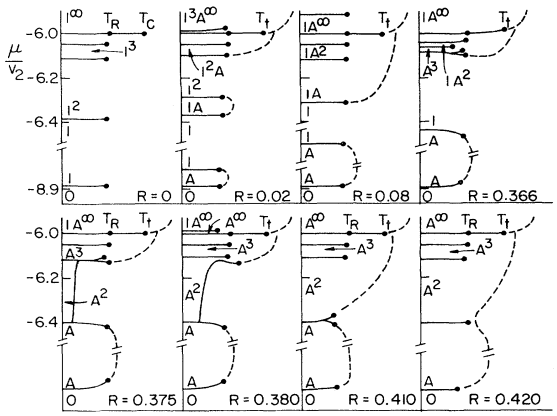

FIG. 8. Surface phase diagrams for strong substrates with weak adatom-adatom repulsion v_1. This sequence, taken with $\alpha=u/v_2=0.75$ held fixed, illustrates the development of narrow epitaxial regions, as v_1 is increased, and their eventual merging into a single epitaxial envelope. Different phases are labeled by their $T=0$ structure. Calculations are exact at $T=0$ and qualitatively correct for $T>0$. Note the breaks in scale of the vertical axes and the omission of the infinite sequence of layer transitions, approaching the bulk phase boundary (cf. Fig. 5). Second-order phase boundaries are shown dotted. Horizontal axis measures T.

pears at $T=0$ for $\beta=5/(f_2-f_3)$, and further epitaxial subregions continue to split off as β increases. The physics here is the successive development and suppression of epitaxy in each surface adlayer: Epitaxial order begins as each layer becomes (roughly) half-filled and is subsequently quenched as the filling process proceeds towards completion. The excess surface density remains finite at all $T>0$. In particular, wetting is incomplete at the bulk transition, because the bulk density is continuous across the bulk phase boundary and the substrate potential does not couple to the (epitaxial) order parameter.[51]

C. Mixed interaction: $0<R<\infty$

Behavior of the phase diagram near the limiting cases discussed above is illustrated in Figs. 8 and 9 for two wetting substrates. Both figures are sketches based on informed interpretation of $T=0$ and mean-field results; however, experience with Monte Carlo comparison suggests that such techniques are a reliable guide to the qualitative evolution of the phase diagram: The major effect of thermal fluctuations[42] (neglected in mean-field theory) is to produce an interfacial roughening temperature T_R. Layer transitions can only occur near bulk coexistence for $T<T_R$ and corresponding layer-transition critical temperatures $T_c(n)$ approach T_R as $n\to\infty$, as discussed in detail in Ref. 14. In Fig. 8 a small repulsive interaction is added to the purely ferromagnetic ($R=0$) strong-substrate layering depicted in Fig. 5(d) with $\alpha=0.75$ held fixed. This causes each first-order layer-transition line to broaden into a narrow epitaxial region. Where the layer transitions are well separated, the regions of epitaxy remain disjoint. Near the bulk phase boundary, however, the ordered regions coalesce into an epitaxial envelope, which encloses a sequence of first-order surface transitions between phases with the $T=0$ structure $[1^kA^m]$, k fixed and $m\to\infty$. Notice the mechanism by which the separated epitaxial regions merge. Increasing the repulsion eventually engulfs all the layering under a single epitaxial boundary. The first-order segment of the bulk phase boundary is always completely wet for $\alpha=0.75$; however, at $R=0.377$ there is a change in $T=0$ coexistence structure (Fig. 4) from $[1A^\infty]$ to $[A^\infty]$. Notice, also, the sequence of transitions *inside* the bulk boundary, corresponding to first-order changes between layer structures of the form $[1^nA^\infty]$. In Fig. 9 a small attractive interaction v_2 is added to the purely antiferromagnetic ($R=\infty$) situation depicted in Fig. 7(a) with $\beta=0.5$ held fixed. As v_2 grows, all the $T=0$ first-order transitions implicit at $v_2=0$ (Fig. 3, Sec. II C) now develop heights $k_BT_c(n)$ which scale as v_2. These layer transitions appear both in the bulk antiferromagnetic phase and under the (surface) epitaxial envelope. Wetting is complete at first-order coexistence for all $0.9196<R<\infty$.

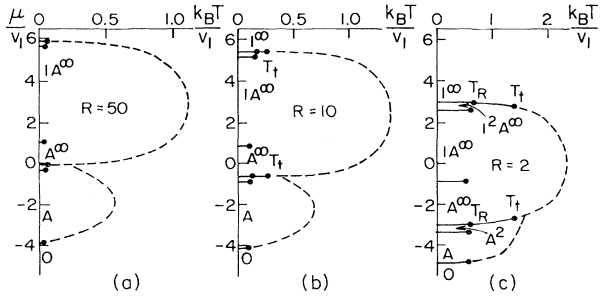

FIG. 9. Surface phase diagrams with weak adatom-adatom attraction v_2. This sequence, taken with $\beta=u/v_1=0.5$ held fixed, illustrates the development of layer transitions in the bulk and surface sublattice-ordered regions. As in Fig. 8, phase boundaries are exact at $T=0$ and qualitatively correct for $T>0$.

So far we have only dealt with strong-substrate behavior, i.e., complete $T=0$ wetting at first-order bulk coexistence. A glance at Fig. 4 reveals two large regions where $T=0$ wetting is incomplete: $\alpha<0.4598$ for all R and the triangular region of structure [1] which includes the point $R=\alpha=0$. Figures 10 and 11 illustrate the systematics along cuts at fixed R, as the strength of the substrate potential is increased (α grows) in such a way as to pass through these regions. Figure 10 ($R=0.2$) is the analog for mixed interactions of Fig. 5: Substrates which are "intermediate" (i.e., not too strong, $\alpha<0.4598$, but not too weak either) have a nonzero wetting temperatures T_W, which may be above T_R (prewetting or critical wetting) or below T_R (layers). In both cases there is now an epitaxial region in the bulk-gas phase for $T>T_W$, within which wetting at coexistence is complete. As the substrate potential is strengthened, T_W goes to zero and layer transitions extend to $T=0$, always under the epitaxial envelope. The epitaxial envelope eventually fissions into subregions, as layers $z=1$, 2, etc., and fill to completion, quenching epitaxy (note the parallels with Figs. 6–8). Figure 11 ($R=10$) starts out for low α similarly to Fig. 10, evolving from intermediate- to strong-substrate behavior, as α grows past $\alpha=0.4598$. Here, however, the effect of making the substrate strong enough to drive the first ($z=1$) layer to completion is to expose the second-layer ($z=2$) adatoms to an unavoidable and strong NN repulsion. This repulsion is so large that the substrate is driven incompletely wet at $T=0$ (layer structure [1] at coexistence) at $\alpha=6.284$ and only becomes completely wet again for $\alpha>11.784$. This constitutes a local reversal of the "normal" (i.e., purely ferromagnetic) tendency[13,14] to wet more readily as u increases, and it will be discussed further in Sec. IV.

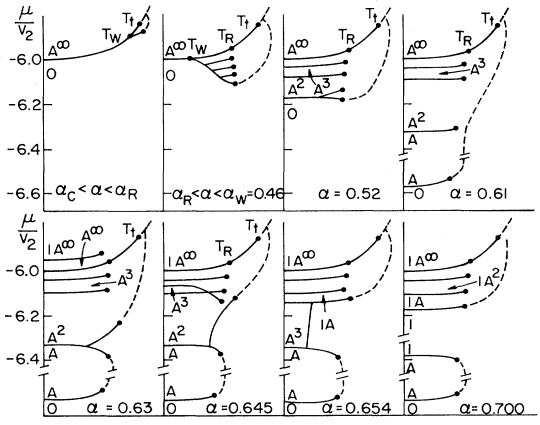

FIG. 10. Surface phase diagrams at $R=v_1/v_2=0.2$, illustrating the effect of increasing substrate attraction ($\alpha=u/v_2$). For $\alpha\gtrsim\alpha_c$ there is a small epitaxial region near T_t. As α increases, T_W decreases, enlarging the epitaxial region. As soon as $T_W<T_R$, layering occurs under the epitaxial envelope. For a strong substrate, the bulk phase boundary is wet even at $T=0$. Eventually the epitaxial envelope fissions as in Figs. 6 and 7. Phase diagrams are exact at $T=0$ and qualitatively correct for $T>0$. High-order layer transitions are omitted. Note breaks in the vertical axes. Horizontal axis measures T.

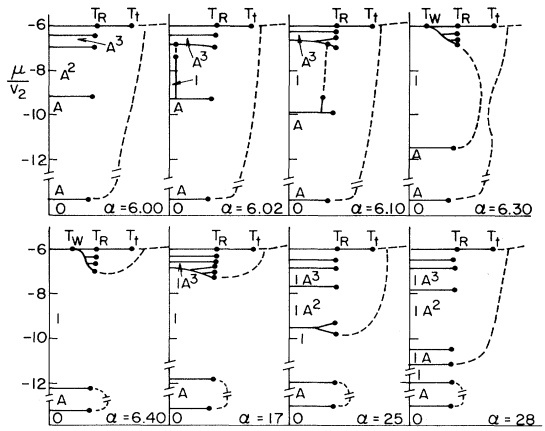

FIG. 11. Surface phase diagrams at $R=v_1/v_2=10$ for a sequence of very strongly attractive substrates. Low-α behavior for $R=10$ parallels that of Fig. 10 and a similar commentary applies. Different phases are labeled by their $T=0$ structure. This sequence illustrates the way the quenching of epitaxy by a very strong substrate can suppress complete wetting, when repulsive adatom-adatom interactions are present. Note, also, the mechanism by which the epitaxial envelope fissions.

Finally, we present in Figs. 12–15 a few samples of detailed Monte Carlo phase-diagram calculations. There is a qualitative correspondence between mean-field and Monte Carlo phase diagrams for similar parameters. Dividing

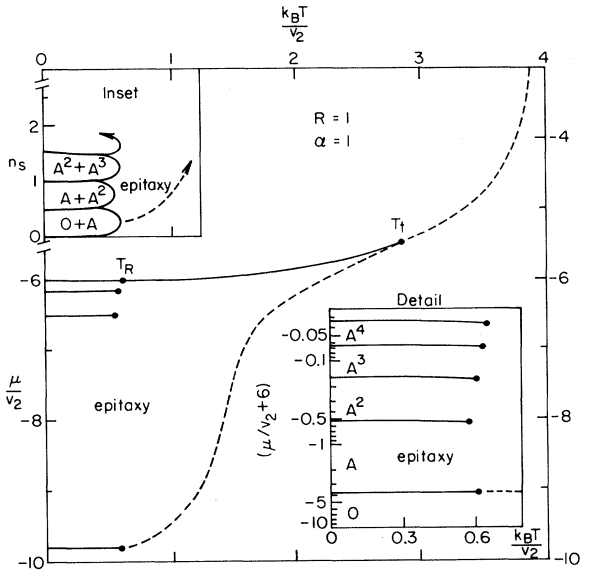

FIG. 12. Surface phase diagram from Monte Carlo calculations for $R=\alpha=1$. Bulk phase boundary is the same as Fig. 1(b). An infinite sequence of layering transitions takes place under the epitaxial envelope near the bulk phase boundary. Because of the space limitation, only the first three transitions are shown in the main figure (and the first five in the detail). Inset at the upper left shows a sketch of the excess surface density $n_s(T)$ [Eq. (2)] along the phase boundaries (same temperature scale as the main figure). Wetting is complete at coexistence for all temperatures below T_t. Second-order boundaries are shown dotted.

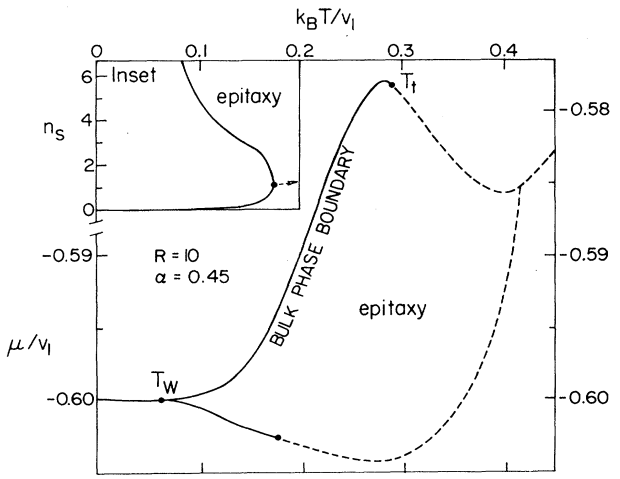

FIG. 13. Surface phase diagram from Monte Carlo calculations for $R=10$ and $\alpha=0.45$. Bulk phase boundary is the same as Fig. 1(c), only greatly enlarged. Notice the rather sharp changes of slope near T_t (Sec. II B). The epitaxial region does not extend down to $T=0$. This is the analog of the prewetting regime for purely attractive interactions. The first-order prewetting line terminates at a tricritical point but has a second-order continuation which completes the epitaxial envelope. Wetting at coexistence is incomplete below T_W. Inset shows excess surface density along the phase boundaries (same temperature scale as main figure).

points between different classes of behavior are, of course, given inaccurately by mean-field theory; however, the sequencing of different types of behavior is generally respected. Only certain rather delicate features, such as those associated with roughening and prewetting,[52] are missed entirely by mean-field theory. Figure 12 shows the

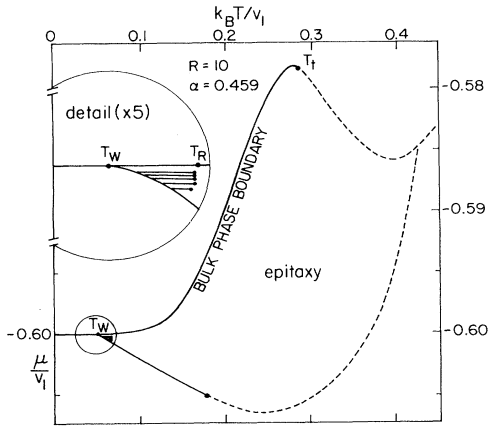

FIG. 14. Surface phase diagram from Monte Carlo calculations for $R=10$ and $\alpha=0.459$. This figure is very similar to Fig. 13. Still the epitaxial region does not extend to $T=0$. Now, however, T_W is less than T_R ($k_BT_R/v_1\approx 0.071$) and layer transitions appear in the epitaxial region. Layer transitions become dense between T_W and T_R along the bulk phase boundary. The first few are shown on an expanded scale in the detail. Note that the wetting temperature here is still quite high, $k_BT_W/v_1=0.0465$, despite the fact that increasing α to 0.4598 sends T_W to zero.

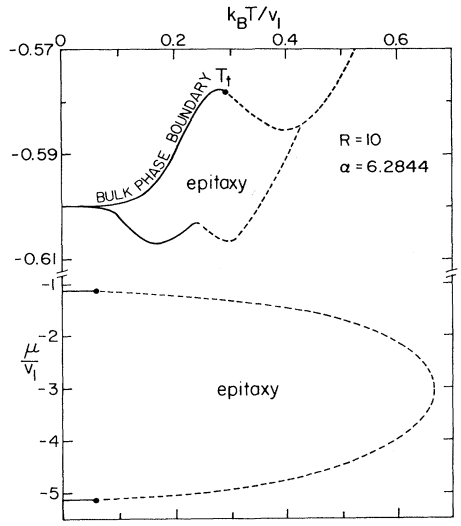

FIG. 15. Surface phase diagrams from Monte Carlo calculations for $R=10$ and $\alpha=6.2844$. This α is just strong enough to produce incomplete wetting at $T=0$ by the strong-substrate dewetting mechanism (Sec. IV A). Epitaxial region is now split into two disjoint subregions, as in Fig. 11 ($\alpha=6.40$).

effects of epitaxy on a typical strong substrate, $R=\alpha=1$, and is qualitatively similar to Fig. 8 ($R=0.420$) and Fig. 9. Layering takes place just as in Fig. 5(d), only now under an epitaxial envelope. The boundary of the epitaxial region uses the first-layer transition ($0\rightarrow A$, first order) and a second-order continuation, which connects with the bulk phase boundary just above T_t. The first- and second-order parts of the boundary join with no change of slope at a surface tricritical[53] point which is just the $d=2$ analog of T_t. Figures 13 and 14 are close to but just below the boundary $\alpha=0.4598$ of the region of complete wetting at $T=0$ (Fig. 4), so there is a nonzero wetting temperature T_W below which wetting is incomplete at coexistence. At $\alpha=0.45$ (Fig. 13), T_W is still above T_R and the system exhibits prewetting behavior [cf., Fig. 5(a) and Fig. 10 for $\alpha_c<\alpha<\alpha_R$]. The first-order prewetting line terminates now at a tricritical point[53] [the analog of the prewetting critical point in Fig. 5(a)] but has a second-order continuation which meets the bulk phase boundary above T_t. At $\alpha=0.459$ (Fig. 14), on the other hand, T_W has become smaller than T_R, so layer transitions appear between T_W and T_R close to the bulk phase boundary [cf. Fig. 5(b) and Fig. 10 for $\alpha_R<\alpha<\alpha_W$]. Finally, Fig. 15 shows the case of $R=10$ with $\alpha=6.2844$, which is just large enough so that the substrate is incompletely wet at $T=0$. Note that the epitaxial region has been split into two separate subregions, as in Fig. 11 ($\alpha=6.40$).

IV. SUMMARY AND DISCUSSION

A. Summary of systematics

The new physical effect introduced by the adatom-adatom repulsion is the stabilization under appropriate

conditions of sublattice ordering. Since there are two sublattices in the simple cubic and square lattices, ordered phases have "antiferromagnetic" Z_2 symmetry, and strongly antiferromagnetic layers are roughly half as dense as completed or nearly completed layers. When considering the bulk-gas region of the surface phase diagram (Fig. 2), the adjacent high-density bulk phase is antiferromagnetic; therefore, filled layers can only form near the substrate and should be thought of as "compressed" (relative to the bulk liquid and/or solid phase) by the substrate attraction. Incompletely wetting films can have a variety of structures with or without such compressed adlayers; however, thick, completely wetting films must always have the structure $[\cdots A^n]$ with $n \to \infty$.

For given physical interactions (i.e., fixed R,α) the T,μ lattice-gas surface phase diagrams in the presence of NN adatom-adatom repulsion do not look dramatically different from their counterparts (Fig. 5) for purely attractive interactions.[13–15] First-order layer transitions are visible whenever wetting at coexistence is complete[54] in any region below T_R. When $T_W > T_R$, prewetting (or critical wetting) occurs. What is new is that (bulk) gas-phase regions exhibiting epitaxy (surface sublattice order) must be separated by a closed phase boundary from nearby disordered regions. This epitaxial envelope may use (first-order) layering and prewetting lines but is completed by additional second-order ("surface antiferromagnetic") boundaries. The epitaxial region may be simply connected or composed of two or more disjoint parts; however, any completely wet part of the bulk phase boundary must be within the envelope of epitaxy, since thick films have $[\cdots A^n]$ structure.

The connectedness of the epitaxial region is controlled by the competing effects of substrate attraction and adatom-adatom repulsion. If repulsion dominates, then an initial ordered (half-filled) layer $[A]$ is stable to compression and the film will tend to grow with the structure $[A^n]$, leading to a connected epitaxial region, as in Figs. 12–14. On the other hand, when substrate attraction dominates, then additional adatoms go into the first layer, forming a compressed structure and "quenching" epitaxy (e.g., Figs. 6 and 7). Epitaxy which is quenched at $T=0$ may be restored by thermal fluctuations at higher temperatures, since the entropy associated with the more open $[A^2]$ structure will in general be larger than that of the compressed [1] structure with the same overall density.[55]

Repulsive interactions can lead, via the quenching mechanism, to wetting systematics which is richer than the purely attractive cases heretofore studied.[13–15] In particular, for $\alpha \lesssim 0.4598$ (Sec. II C) the usual rule applies: A stronger substrate has more tendency to wet. However, for an appropriate range of positive R, further increasing the substrate strength *dewets* the substrate, and complete wetting is only restored for still-stronger substrates. The mechanism for this "strong-substrate dewetting" is that the formation of the quenched, compressed first layer [1] exposes the full second layer to NN repulsion, thus forming an *effective substrate* (the bare substrate plus the first layer) for the second and subsequent layers which no longer wets at $T=0$.

B. Commentary

Any connection between this model and the properties of specific adsorbate/substrate systems is likely to be indirect; nevertheless, certain generic properties of real systems can perhaps be illuminated by the model. The lattice-gas model makes the bulk "solid" commensurate with the epitaxial phase, whereas in practice there is no reason for the bulk lattice parameter to match that of a physical epitaxial phase. Thus, while submonolayer epitaxy is common,[1–6,24] thicker solid films are normally incommensurate,[56] so there are *at least* three (rather than two) relevant surface symmetries, epitaxial, substrate-commensurate ("fluid") and incommensurate ("$d=2$ solid"). Of course, nonspherical adatoms have additional degrees of freedom, and real systems such as oxygen[57,58] apparently exhibit many additional surface phases, involving orientational ordering, different $d=2$ space-group symmetries, etc.

Another feature which our lattice model lacks is the possibility of several different high-density *bulk* phases which can coexist with the (bulk) gas phase. The simplest example of this is the usual liquid-solid distinction; in addition, materials such as O_2 have several different solid phases. When these bulk phases are separated by first-order transitons, a variety of triple points may appear. Surface behavior in the vicinity of such bulk triple points is just beginning to be studied.[35] Because triple points are first order, coexistence singularities such as T_R and T_W do not move through them smoothly (as a function of interaction parameters) and may easily get trapped.[59] For example, the liquid-gas phase boundary is always rough, so, when gas-solid coexistence happens to be smooth everywhere, that leaves the gas-liquid-solid triple point as an effective roughening temperature.

Despite these shortcomings, the lattice gas does model in a generic, and, we hope, a useful way certain real-world behavior. We conclude with three remarks.

1. *Lateral ordering and film buildup*

Our results suggest that, for a given adatom/substrate pair, film-buildup transitions proceed more or less independently of lateral-ordering transitions. Regions of different lateral symmetry may or may not be connected; the boundaries between them may or may not use the layering and/or prewetting lines associated with film buildup. The overall picture can be quite complex (Figs. 8–10). There is no experimental system that we are aware of for which the surface phase diagram has been completely mapped out; however, none of the above statements is inconsistent with what is presently known about, for example, O_2 or C_2H_4 on graphite.[57,58,60,61]

2. *Epitaxial quenching*

A close analog of epitaxial quenching is, in fact, very common in systems exhibiting submonolayer epitaxial phases: Epitaxial phases (such as the $\sqrt{3}\times\sqrt{3}$ phase of He/graphite)[24] which form at intermediate coverage are ordinarily succeeded at higher coverage by the incom-

mensurate solid. The relatively high-density incommensurate phase here plays the role of the compressed phase in the lattice gas. The principal difference is that in the lattice gas the compressed phase has the same symmetry as the ($d=2$) gas (i.e., that of the substrate), while the incommensurate solid phase has a symmetry distinct from that of the substrate.

3. *Strong-substrate dewetting*

Recent RHEED measurements by Seguin *et al.*[18] demonstrate that Ar and Xe completely wet graphite at low temperatures, while Ne and N_2 do not. Examination of van der Waals parameters for these systems[18] shows that the ratio of atom-atom to atom-substrate attraction ($\alpha=u/v_2$ in the lattice model) is larger for Ne and N_2 than for Ar and Xe. Viewed from the perspective of purely attractive models,[13,14] this is paradoxical. A possible explanation[18] is suggested by the strong-substrate dewetting phenomenon: Ar and Xe on graphite may be "normal" strong-substrate systems, while the stronger-substrate systems Ne and N_2 may "dewet" due to the formation of one or more compressed early layers by a mechanism closely related to what happens in the lattice model. The physical picture is that the compression (*not* here related to quenching of epitaxy, since the van der Waals core is very hard and all these systems form incommensurate solids in the region in question) produces a misfit of lattice parameters between the early layers and the potential bulklike wetting layers above. In order for a thick film to form, this misfit must be healed out by some dislocation structure which interpolates between the tightly bound, compressed layers and the overlayers. The (free) energy cost of this misfit (i.e., the energy of the dislocation network) plays the role of the repulsive interaction to which the second layer is exposed in the lattice model. If the compression is too great, then the energy cost is high and overlayers do not form, i.e., dewetting occurs. Thus, the energy cost of the misfit acts as a negative (repulsive) contribution to the attraction of the "effective substrate" consisting of the real substrate plus the tightly bound, compressed early layers. A direct test of this hypothesis using van der Waals parameters and experimental layer structure is now in progress.[62]

ACKNOWLEDGMENTS

We have enjoyed and benefited from discussions with M. Bienfait, R. J. Birgeneau, J. G. Dash, P. M. Horn, C. Jayaprakash, Y. Lahrer, D. P. Landau, S. Leibler, R. Lipowski, P. Nightingale, R. Pandit, W. F. Saam, and M. Schick. One of us (M.W.) wishes to acknowledge the hospitality of the Department of Theoretical Physics, Centre d' Etudes Nucléaires, Saclay, where part of this paper was written. This work was supported in part by the National Science Foundation under Grant Nos. DMR-80-20250 and DMR-81-17182.

[1]J. G. Dash, *Films on Solid Surfaces* (Academic, New York, 1975).

[2]*Phase Transitions in Surface Films,* edited by J. G. Dash and J. Ruvalds (Plenum, New York, 1980).

[3]M. Bienfait, in *Current Topics in Materials Science,* edited by E. Kaldis (North-Holland, New York, 1979).

[4]A. Thomy, X. Duval, and J. Regnier, Surf. Sci. Rep. 1, 1 (1981).

[5]*Ordering in Two Dimensions,* edited by S. K. Sinha (North-Holland, New York, 1980).

[6]K. Binder, in Phase Transitions and Critical Phenomena, edited by C. Domb, M. S. Green, and J. L. Lebowitz (Academic, New York, in press).

[7]When the bulk phase is not a fluid, n_b becomes a function of z and $\vec{\rho}$, so this discussion must be generalized; however,

$$n_s \equiv \lim_{S\to\infty} \frac{1}{S} \int_S (d^2\rho) \int_0^\infty dz [\langle n(z,\vec{\rho})\rangle - n_b(z,\vec{\rho})]$$

remains well defined.

[8]In experiments the pressure P is often a more accessible equivalent to μ.

[9]C. Ebner and W. F. Saam, Phys. Rev. Lett. 38, 1486 (1977).

[10]J. W. Cahn, J. Chem. Phys. 66, 3667 (1977).

[11]M. J. de Oliveira and R. B. Griffiths, Surf. Sci. 71, 687 (1978).

[12]M. Wortis, R. Pandit, and M. Schick, in *Melting, Localization and Chaos,* edited by R. Kalia and P. D. Vashishta (North-Holland, New York, 1982), p. 13.

[14]R. Pandit, M. Schick, and M. Wortis, Phys. Rev. B 26, 5112 (1982), which contains numerous additional references, both theoretical and experimental.

[15]H. Nakanishi and M. E. Fisher, Phys. Rev. Lett. 49, 1565 (1982).

[16]D. M. Kroll and R. Lipowski, Phys. Rev. B 26, 5289 (1982), and unpublished. See also R. Lipowski, Phys. Rev. Lett. 49, 1575 (1982); Z. Phys. B 51, 165 (1983).

[17]E. Brézin, B. I. Halperin, and S. Leibler, J. Phys. (Paris) 44, 775 (1983).

[18]J. L. Seguin, J. Suzanne, M. Bienfait, J. G. Dash, and J. A. Venables, Phys. Rev. Lett. 51, 122 (1983).

[19]M. E. Fisher and G. Caginalp, Commun. Math. Phys. 56, 11 (1977).

[20]R. B. Griffiths, in *Phase Transitions in Surface Films,* Ref. 2.

[21]M. P. M. den Nijs (unpublished).

[22]The destruction of an epitaxial phase by thermal fluctuations is not "melting" in our terminology. Incommensurate solid melting may be either first or second order.

[23]B. I. Halperin and D. R. Nelson, Phys. Rev. Lett. 41, 121 (1978); D. R. Nelson and B. I. Halperin, Phys. Rev. B 19, 2456 (1979); S. T. Chiu, in *Melting, Localization, and Chaos,* edited by R. Kalia and P. D. Vashishta (North-Holland, New York, 1982), p. 29.

[24]*Monolayer and Submonolayer Helium Films,* edited by J. G. Daunt and E. Lerner (Plenum, New York, 1973). For more recent work see R. E. Ecke and J. G. Dash, Phys. Rev. B 28,

3738 (1983) (see especially Fig. 14).
[25]Commensurate-incommensurate transitions can, of course, be studied via appropriate lattice models. See, for example, M. Kardar and A. N. Berker, Phys. Rev. Lett. 48, 1552 (1982).
[26]*Phase Transitions and Critical Phenomena,* edited by C. Domb and M. S. Green (Academic, London, 1974), Vol. 3, p. 425.
[27]D. M. Burley, Physica 27, 768 (1961).
[28]Z. Racz, Phys. Rev. B 21, 4012 (1980).
[29]K. Motizuki, J. Phys. Soc. Jpn. 14, 759 (1959).
[30]J. M. Kincaid and E. G. D. Cohen, Phys. Lett. 50A, 317 (1974); Phys. Rep. 22, 57 (1975).
[31]R. Bidaux, P. Carrara, and B. Vivet, J. Phys. Chem. Solids 28, 2453 (1967).
[32]The effect of fluctuations is even stronger in $d=2$. E. Müller-Hartmann and J. Zittartz, Z. Phys. B 27, 261 (1977).
[33]H. J. Herrmann, E. B. Rasmussen, and D. P. Landau, J. Appl. Phys. 53, 7994 (1982).
[34]Indeed, as Figs. 12 and 13 show, the slope of the phase boundary $d\mu/dT$ may change sign in a narrow region near and above T_t.
[35]An appropriate Potts lattice gas can, however, show three bulk phases and a triple point. C. Ebner, Phys. Rev. B 28, 2890 (1983).
[36]It is, of course, a restriction of the lattice model that the atom-atom hard-core exclusion matches the substrate periodicity (see Sec. IV A).
[37]Complete wetting is also related to Antonov's rule and to the possibility of crystallite growth on the substrate (Ref. 14). See also B. Widom, J. Chem. Phys. 62, 1332 (1975); W. L. Winterbottom, Acta. Metallurg. 15, 303 (1967).
[38]D. E. Sullivan, D. Levesque, and J. J. Weis, J. Chem. Phys. 72, 1170 (1980).
[39]K. Binder and P. C. Hohenberg, Phys. Rev. B 6, 3461 (1972); B 9, 2194 (1974).
[40]C. Ebner, Phys. Rev. A 22, 2776 (1980).
[41]R. Pandit and M. Wortis, Phys. Rev. B 25, 3226 (1982).
[42]For a review of the roughening literature, see J. D. Weeks, in *Ordering in Strongly Fluctuating Condensed-Matter Systems,* edited by T. Riste (Plenum, New York, 1980), pp. 293–317. Note that the statement refers to the effect of fluctuations on the *global* structure of the phase diagram. Of course, such fluctuations can also produce important *local* effects on critical behavior (see, e.g., Ref. 17).
[43]What follows is a transcription to the lattice-gas language of the mean-field theory for magnetic surfaces. See, for example, Refs. 36–38.
[44]R. Fletcher and C. M. Reeves, Comput. J. 7, 149 (1964).
[45]C. Ebner, Phys. Rev. A 23, 1925 (1981).
[46]Continuum (Landau-Theory) approaches such as Ref. 12 and, for example, G. F. Teletzke, L. E. Scriven, and H. T. Davis, J. Coll. Interface Sci. 87, 550 (1982), give wetting systematics but no discrete layer transitions.
[47]I. M. Kim and D. P. Landau, Surf. Sci. 110, 415 (1981).
[48]W. F. Saam, Surf. Sci. 125, 253 (1983).
[49]M. P. Nightingale, M. Schick, and W. F. Saam (unpublished).
[50]The particular forms of Figs. 5(b) and 5(c) depend on the long range of the substrate potential $u(z)\sim 1/z^3$.
[51]Of course, n_s is singular at the bulk second-order transition, presumably as $n_s\sim n_s^0+(\mu_c-\mu)^\tau$ with $\tau>0$.
[52]In mean-field theory layer transitions are always present with $T_c(n)\rightarrow T_c$ (bulk) (Ref. 14) instead of $T_c(n)\rightarrow T_R$; thus, the characteristic behavior for $T_W>T_R$ (prewetting, critical wetting) is missing.
[53]Main-field theory gives surface critical-endpoint structure for sufficiently large R, as discussed for the bulk in Sec. II B. Fluctuations appear to restore tricritical behavior; however, as in $d=3$, available data show small slope anomalies for large R and the situation remains uncertain.
[54]The visibility of the layer transitions and the fact that $T_c(n)\rightarrow T_R$ as $n\rightarrow\infty$ provides a method for determining the roughening temperature. Of course, T_R is an interfacial property of the adatoms alone, so its value does not depend on the substrate. However, from a practical point of view it is often easier experimentally to measure T_R indirectly via layer transition on a strong substrate than directly as a interfacial property. For example, the measurements of S. Ramesh and J. D. Maynard [Phys. Rev. Lett. 49, 47 (1982)] on ^{4}He/graphite determine the roughening temperature of the hcp solid-superfluid interface.
[55]It is for this reason that the quenched region grows up from $T=0$ in Figs. 6 and 7. Note, however, that the argument is strictly true only when the transition is second order, so that behavior like Fig. 11 ($\alpha=6.02$) is not excluded.
[56]See, for example, the effects of incommensurability as studied by F. Millot, Y. Lahrer, and C. Tessier, J. Chem. Phys. 76, 3327 (1982), and other references therein.
[57]P. W. Stephens, P. A. Heiney, R. J. Birgeneau, P. M. Horn, J. Stoltenberg, and O. E. Vilches, Phys. Rev. Lett. 45, 1959 (1980).
[58]D. D. Awschalom, G. N. Lewis, and S. Gregory (unpublished).
[59]M. Schick and M. Wortis (unpublished).
[60]J. Menaucourt, Ph.D. thesis, Université de Nancy, 1977 (unpublished).
[61]J. Menaucourt, A. Thomy, and X. Duval, J. Phys. (Paris) Colloq. 38, C4-195 (1977).
[62]M. Schick, private communication.

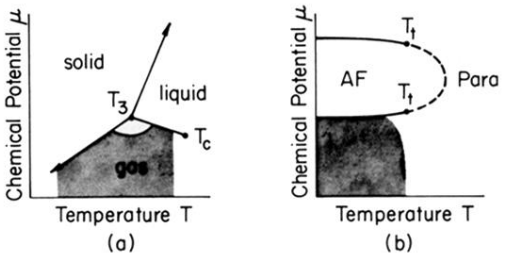

FIG. 2. Comparison of the bulk phase diagrams of (a) the continuum gas-liquid-solid system and (b) our lattice gas with competing interactions. The lattice gas has only two phases and lacks a triple point. The continuum system has no extended second-order phase boundary. However, surface behavior in the shaded regions may be analogous, as explained in the text.